

Article

# Investigation of CO<sub>2</sub> Variation and Mapping Through Wearable Sensing Techniques for Measuring Pedestrians' Exposure in Urban Areas

Ilaria Pigliautile <sup>1</sup>, Guido Marseglia <sup>1,2</sup> and Anna Laura Pisello <sup>1,3,\*</sup> 

<sup>1</sup> CIRIAF, University of Perugia, 06125 Perugia, Italy; pigliautile@crbnet.it

<sup>2</sup> Research Department, Link Campus University of Rome, 00165 Rome, Italy; g.marseglia@unilink.it

<sup>3</sup> Department of Engineering, University of Perugia, 06125 Perugia, Italy

\* Correspondence: anna.pisello@unipg.it; Tel.: +39-075-585-3563

Received: 6 February 2020; Accepted: 6 May 2020; Published: 11 May 2020



**Abstract:** Citizens' wellbeing is mainly threatened by poor air quality and local overheating due to human-activity concentration and land-cover/surface modification in urban areas. Peculiar morphology and metabolism of urban areas lead to the well-known urban-heat-island effect, characterized by higher air temperature in cities than in their surroundings. The environmental mapping of the urban outdoors at the pedestrian height could be a key tool to identify risky areas for humans in terms of both poor-air-quality exposure and thermal comfort. This study proposes urban environment investigation through a wearable miniaturized weather station to get the spatial distribution of key parameters according to the citizens' perspective. The innovative system monitors and traces the field values of carbon dioxide (CO<sub>2</sub>) concentration, such as air temperature and wind-speed values, which have been demonstrated to be related to outdoor wellbeing. The presented monitoring campaign focused on a two-way, two-lane road in Rome (Italy) during traffic rush hours on both working days and weekends. Collected data were analyzed with respect to timing and position, and possible correlations among different variables were examined. Results demonstrated the wearable system capability to catch pedestrian-exposure variability in terms of CO<sub>2</sub> concentration and local overheating due to urban structure, highlighting potentials in the citizens' involvement as observation vectors to extensively monitor urban environmental quality.

**Keywords:** microclimate; CO<sub>2</sub> monitoring; urban heat island; monitoring; wearable sensing; outdoor comfort

## 1. Introduction

World urban-population growth and urban built-up expansion are internationally recognized and consolidated trends [1], particularly intense in developing countries [2]. This demographic tendency means that an increasing number of people will live in urban areas where impervious surfaces generally replace natural ground, altering local energy balance [3,4]. Increasing concentration of anthropogenic actions and activities is further responsible for air-quality deterioration and contributes to local overheating [5,6]. In this view, in 2015, the Member States of the United Nations committed to implementing the 2030 Agenda for Sustainable Development [7], including the economic, social, and environmental fields of sustainable development. The Agenda is based on 17 universal Sustainable Development Goals (SDGs), aimed at reducing inequality and improving living standards all around the globe, and always keeping high attention on sustainability [8]. The urban sustainability concept is thus gaining increasing attention among the scientific community and urban planners, as reported by Shen et al. [9]. Within this framework, governments have to promote urgent actions to fight climate

change and its impact on humans' life quality and well-being, and the improvement of urban air quality is a key point in achieving the proposed SDGs [10–14].

Regarding the pollutant emissions, some research has underlined that transport (including the movement of people and goods by cars, trucks, trains, ships, airplanes, and other vehicles) is one of the main sectors for the emission of the Greenhouse Gases (GHGs) [15]. Garceau [16] demonstrated, through long-term monitoring of air pollutants, that introduction of roundabouts allowed decreasing PM<sub>2.5</sub> concentrations up to 40% in the case study of Kneehill, New Hampshire (USA). The municipality of Potsdam (Germany) introduced specific traffic-reducing measures in 2017, and Schmitz et al. [17] investigated the public acceptance of the implemented actions by means of questionnaire submission. The study highlighted that individual awareness of the air-quality problem was the most important predictor of community support. Moreover, the European Commission has defined an important CO<sub>2</sub> vehicle-emission-reduction project, setting the limit value for the New European Driving Cycle (NEDC) of 95 g/km of CO<sub>2</sub> to be reached before 2021 [18].

Urban areas, and thus citizens, are particularly vulnerable to pollutant exposure since the urban form alters wind patterns, producing wind-calm or vortex zones [19], and pollutant sources are mainly concentrated in urbanized areas, such as vehicular traffic, industrial activities, heating systems, and commercial areas. Thanks to rising awareness and recent emission-reduction standards, important improvements have been achieved worldwide in terms of air quality, but pollutant-concentration limit values still exceed the Air-Quality Standards' threshold values in several cities [20–23]. These standards mainly focus on PM<sub>10</sub>, PM<sub>2.5</sub>, NO<sub>x</sub>, and SO<sub>x</sub> concentration monitoring, while CO<sub>2</sub> is not commonly mentioned as a pollutant since it is harmful to human beings only at very high concentration levels, that is, equal to or above 2%, as specified by Langford [24]. Nevertheless, high CO<sub>2</sub> emissions cause severe damage to human health [25–27], and variations of its concentration levels below the urban canopy could represent the existence of punctual anthropogenic sources which may be threatening the environmental quality of the outdoors. Accordingly, CO<sub>2</sub> concentration could be assumed as representative of the air quality [28].

Furthermore, cities are affected by the well-known phenomenon of the Urban Heat Island (UHI) [29,30] due to their morphological peculiarities, land surface cover and usage, and lack of greenery [31]. This specific microclimate characteristic mainly occurs in the higher air temperatures detected in the urban areas with respect to rural surroundings, but it also further deteriorates the air quality of urban spaces, altering city photochemistry [32] and affecting atmospheric circulation [33]. The relationship between microclimate features, such as air temperature, solar radiation, wind speed, air pollution, and urban morphology, can be understood through a detailed analysis of the temporal and spatial distribution of the Urban-Heat-Island Intensity (UHII) [34] which numerically expresses the impact on microclimate due to urban environment. High values of UHII compromise citizens' everyday commuting, open-air activities, and dwellers' well-being, in general [35,36].

Zhang et al. [37] considered a diagnostic methodology to evaluate the UHI effect in Xi'an, a Chinese city. They proposed a model to estimate the maximum UHI intensity on the basis of real meteorology data of a rural station, analyzing the link between UHI and the city morphology. Pakarnseree et al. [38] highlighted the importance of considering, in buildings, such physical features as the Water Surface Ratio (WSR), Street Surface Ratio (SSR), Park Surface Ratio (PSR), Building Coverage Ratio (BCR), and Floor Area Ratio (FAR) that strongly influence the presence of the UHI issue in the Bangkok area. Li et al. [39] underlined the interaction between the UHI and the Urban Pollution Island (UPI) by analyzing their effects on the environment during summer in Berlin, focusing on various risky aspects that made citizens more vulnerable during hotter seasons. Rizvi et al. [40] showed the existence of UHI in a city in the Pakistan zone and analyzed the effects of its interaction with Heat Waves (HWs) which are foreseen to be more intense and frequent in the next decades due to climate change [41]. The sensitivity of the existing synergy between HWs and UHI was investigated through climate modelling by Zhao et al. in [42], even in future climate scenarios. The relationship between microclimate parameters in urban zones and the effects of global warming were analyzed by Sun et al. [43]. Gu and

Li [44] evaluated the impact of precipitation on the intensity of UHI in the continental United States at microclimate scales. Jato-Espino [45] analyzed the impact of UHI in the Mediterranean area by means of statistical analysis, considering the value of the daily thermal fluctuations.

The common practice of urban environmental monitoring is conducted by means of fixed monitoring-station networks [46,47] properly designed in order to optimize monitoring costs, that is, the instruments, installation and maintenance, and spatial coverage [48]. Nevertheless, the high heterogeneity of city landscapes leads to highly granular microclimatic conditions which could not be detected by those networks due to their dimensions [49]. Furthermore, weather stations are generally located above roof levels, and such position does not allow to catch the pedestrians' perspective in the urban environment, losing information for an accurate evaluation of citizens' life quality and well-being. Spatial distribution of anthropogenic activities, which could be assumed as punctual or linear sources of pollutants, produces different air quality levels at the pedestrian height throughout cities [50] that could not be highlighted from common station networks either.

Therefore, experimental data collection below the urban canopy is fundamental to map the urban environment in terms of site-specific microclimate conditions and air-quality personal exposure. To guarantee citizens' health and security, the current challenge is to study more and more sophisticated monitoring systems and methods for real-time evaluation of the urban-microclimate spatial pattern.

Nowadays, the scientific community is moving in this direction, focusing on collecting environmental data at a high spatial resolution, taking advantage of advances in technology and communication sectors [51–53]. Dominguez et al. [54] developed a cloud platform to integrate different typologies of environmental-sensor networks with a sensor web providing urban air and noise pollution data to common citizens. Pedestrians can thus decide how to move around the city on the basis of pollutant spatial distribution, as proposed by Dhingra et al.'s IoT-Mobair application [55].

Considering this scenario, the current work moved from previous contributions of the authors [56–58] to further investigate monitoring potentials of an experimental innovative system in terms of urban CO<sub>2</sub>-level mapping. In particular, CO<sub>2</sub> concentration was assumed as an indicator of existing anthropogenic activities in the investigated area [59] that may affect the environmental quality at the pedestrian height which cannot be highlighted by common fixed monitoring stations. Taking advantage of the improvements in wearable sensing techniques [60], pedestrians became predominant observational vectors allowing to accomplish a twofold aim: (i) to increase monitoring network coverage, and (ii) to focus data collection on humans exposed to urban environmental conditions. In particular, the developed system was a miniaturized weather station which could be settled on a common bike helmet due to its small size and light weight. The adoption of a wearable sensing technique also allowed to monitor the quality of the urban environment across areas which were not approachable by vehicles that were the most common observation vectors. Moreover, the monitoring perspective was that of the pedestrian, thus data collected through this method were strictly related to the real perception of dwellers living in the outdoor spaces of the city. As the key research progress with respect to previous works, here the focus was also on CO<sub>2</sub>-concentration mapping through wearable sensing techniques, which are considered to be an innovative tool for identifying air quality as specifically perceived by pedestrians in dense and polluted urban areas [61]. In addition, CO<sub>2</sub> concentration, even at a very local scale, may be correlated to an increase in premature mortality. CO<sub>2</sub> local increase in concentration was indeed correlated to an increase in ozone concentration and particulate matter. In this view, even more importantly, specific granular, localized CO<sub>2</sub>-concentration-mitigation strategies may also be helpful in reducing local air-pollution mortality, even if CO<sub>2</sub> is not specifically controlled in adjacent regions [62].

The experimental set-up with the basic information on the prototype design, embedded sensors accuracy and system recording mode, and a description of the planned monitoring for the CO<sub>2</sub> concentration analysis across the case study area are presented in Section 2. The monitoring system was tested by planning a monitoring campaign focused on the limited area of Rome (Italy) which is described in Section 3. Finally, the obtained monitoring results are discussed, showing detected CO<sub>2</sub>

spatial distribution and pointing out correlations among the monitored gas particles, other collected environmental parameters, and site-specific characteristics.

## 2. Material and Methods

The experimental campaign focused on a heavy-traffic urban road which was monitored during peak rush hours, i.e., around 9:30 a.m. and 6:30 p.m., by means of a miniaturized weather station settled on a common bike helmet. The observer was always the same person throughout the whole monitoring campaign, thus the worn station was always at the same height, i.e., sensors platform was at about 180 cm in height, and the walking speed was kept constant as much as possible going along the selected road from A to B and backward. The designed monitoring system and the planned monitoring campaign are described in the following subsections.

### 2.1. Monitoring System

The monitoring system was a miniaturized weather station specifically designed in order to be worn by pedestrians or city bikers and thus to catch the perspective of these weak categories within the urban environment. The system monitored the main environmental parameters such as air temperature, relative humidity, wind speed and direction, solar radiation, illuminance level, and CO<sub>2</sub> concentration. Table 1 reports technical specifications of the embedded sensors in terms of data accuracy which was acceptable considering the small size of the whole system.

**Table 1.** Technical specifics of the embedded sensors.

Monitored Parameter	Technical Specifications
Air Temperature (Ta) [°C]	Operation range: $-40 < Ta < +85^{\circ}\text{C}$ Absolute accuracy: $\pm 0.5^{\circ}\text{C}$ at $25^{\circ}\text{C}$
Relative Humidity (RH) [%]	Absolute tolerance: $\pm 3\%$
Atmospheric Pressure (Pa) [hPa]	Operation range: $300 < Pa < 1100$ hPa Sensitivity error: $\pm 0.25\%$
Global Solar Radiation (SR) [ $\text{W}/\text{m}^2$ ]	Spectral range: $360 < SR < 1120$ nm Calibration uncertainty: $\pm 5\%$
Lighting (E) [lux]	Spectral error: $2.3\%$
Wind Speed (ws) [m/s]	Operational range: $0.25 < E < 40$ m/s Resolution: 0.1 m/s Sensitivity: 0.13 m/s
Wind Direction (wd) [deg]	Resolution: $1^{\circ}$ Sensitivity: $\pm 1^{\circ}$
CO <sub>2</sub> Concentration (CO <sub>2</sub> ) [ppm]	Accuracy: $\pm 2\%$ full scale at $20^{\circ}\text{C}$ and 1000 hPa

Data were collected every two seconds, and each observation was associated with GPS coordinates, i.e., latitude, longitude, elevation, and attitude (roll, pitch, and yaw). The GPS horizontal spatial accuracy was 2.5m. The operator communicated with the system through a Wi-Fi access point which was automatically generated by the system when it was switched on. The Wi-Fi connection allows to check data in real time and manage data-recording sessions from a smartphone or other portable device. The authors have already presented the monitoring system validation and its potentials in detecting critical conditions for citizens in terms of thermal comfort in [56,57].

### 2.2. Monitoring Campaign and Data Analysis

The monitoring campaign aimed to statistically characterize a heavy-traffic urban road in terms of CO<sub>2</sub> concentration according to the pedestrian perspective.

In this view, the designed campaign consisted of several repetitions of the same path in different days in order to compute means and fluctuations of the parameter in the specific area and thus to verify the monitoring system's capability in detecting CO<sub>2</sub> punctual or linear sources, most probably related to intense anthropogenic activities in urban contexts [58]. All the monitoring sessions were carried out

during the same month (March 2019) to avoid a significant effect of collected data fluctuation due to the seasonal cycle of the gas.

In particular, the observer covered the same path from point A to point B and backward along the selected road several times throughout the month, always during traffic rush hours, i.e., around 9:30 a.m. and 6:30 p.m. The presented monitoring campaign comprised 16 continuously monitored transects consisting of eight sessions at 9:30 a.m. and eight sessions at 6:30 p.m.; five out of the 16 conducted sessions concerned weekend days, as summarized in Table 2. In this way, a comparative assessment of the two traffic-dependent conditions was possible.

**Table 2.** Performed monitoring sessions.

Time	Number of Monitoring Sessions		
	9:30 a.m.	6:30 p.m.	
Weekdays	6	5	11
Weekend days	2	3	5
	8	8	Total: 16

The monitoring repetitions allowed to collect a significant amount of data and to analyze both the background level and the events-related spatial distributions of the analyzed gas. In particular, datasets collected during each monitoring session were analyzed in terms of detected minimum and maximum values, and the average and standard deviation of the data distribution. The same statistical analysis was performed on the whole collected population of data and two data partitions outlined following two different criteria: (i) morning and afternoon campaigns, and (ii) weekdays and weekends.

Finally, correlations between detected CO<sub>2</sub> concentration and other environmental parameters, i.e., air temperature and wind speed, were investigated since possible significant dependencies would support the analysis of the CO<sub>2</sub>-level dispersion throughout the monitored area. All the presented data were simultaneously collected by the same wearable station described in the previous section.

### 3. Case Study

The case study was selected in order to be a relatively “short” transect of the city that could be (i) easily accessible by the researcher wearing the system and (ii) covered in a limited time span in order to avoid time-related fluctuations of the monitored parameters in each single monitoring session. Furthermore, the selected area had to present a clearly defined morphology, i.e., unique orientation and almost-constant aspect ratio, in order to avoid any possible fluctuations of the parameter which could be imputed to different configurations of the crossed area. All the observed variations were thus to be imputed to punctual sources existing in the area or to mutual dependencies among different environmental parameters.

Given the presented constraints, the specific case study was in a moderately polluted area, according to the reports of the Regional Environmental Protection Agency [63], connecting one of the two main railway stations in Rome to one of the functional hubs of the city.

The case study comprised two carriageways, both of two lanes covering a road of 450 meters in length in Rome (Italy) and connecting two squares which were generally congested during traffic rush hours, around 9:30 a.m. and 6:30 p.m. The monitoring path started and finished in the Southern square. The operator covered both the roadsides and a single monitoring session comprising forward and backward routes, i.e., total length of each session of about 900 meters. The walking average speed was 6 km/h, and it ensured a dataset of about 260 observations for each performed session. Figure 1a and b shows the monitored area scheme and the conducted monitoring campaign, respectively.

The monitored road intersected at two points by secondary roads. These were one-way, one-lane streets, and both intersections with the main road under study were regulated by traffic lights. Therefore, it was common to face frequent acceleration and deceleration of traffic speed along the selected road with a consequent increment of vehicle emissions in the area.

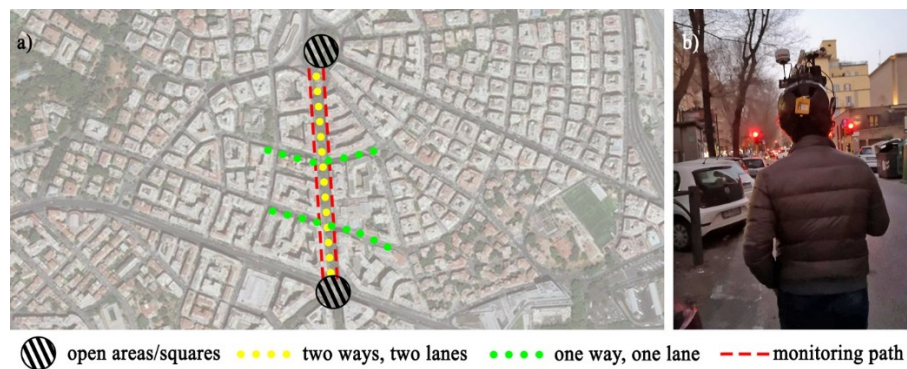


**Figure 1.** (a) Monitored area scheme; (b) conducted monitoring campaign.

#### 4. Results and Discussion

Human exposure to varying carbon dioxide concentration was investigated in terms of CO<sub>2</sub> geospatial distribution and combining detected pollutant levels with air temperature and wind speed monitored data. In particular, CO<sub>2</sub> concentration analysis was correlated with each specific session of monitoring, day of the week (weekends and working days), timing during the course of the day, and position along the path, with particular attention to crossroads points, which have been demonstrated to exacerbate pedestrians' wellbeing, as showed in previous studies [64]. In detail, Figure 2 shows the spatial distribution of the collected CO<sub>2</sub> concentration along the monitored route for each monitoring session, both forward and backward. Evident massive variability of carbon-dioxide-concentration levels was visualized by means of the proposed techniques. Monitoring sessions 1 and 2 (both tests) and monitoring session 6 in the afternoon refer to weekends showing a relatively weaker anthropogenic pressure, compared to most weekdays. Non-negligible local increase of concentration was focused in specific spots with no clear instant correlation to crossroads (highlighted sections) and in specific peak times, even within the same monitoring round. Results demonstrated how highly detailed and granular data are required to be integrated into classic weather stations' data, since the variability of air-quality related parameters was strongly affected by the local and temporary phenomena, affecting pedestrians' wellbeing.

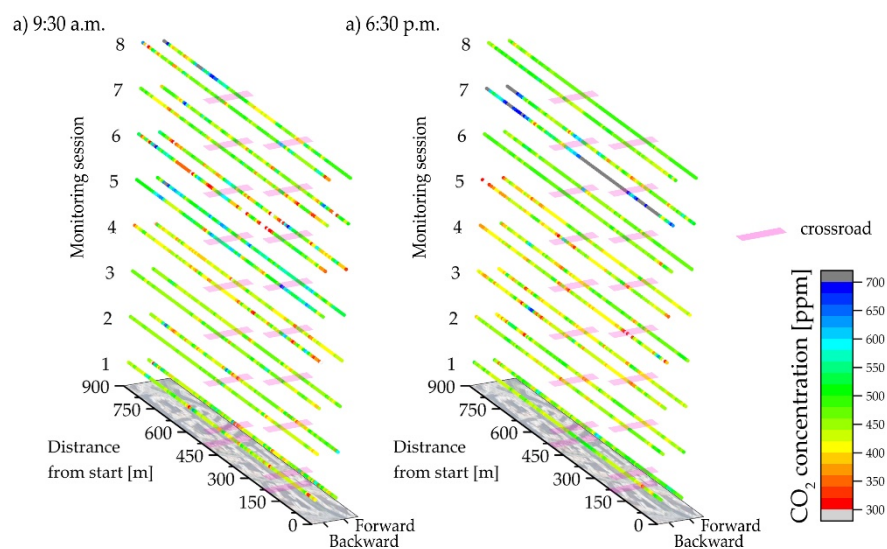


**Figure 2.** Spatial distribution of CO<sub>2</sub> concentration as collected during the performed monitoring sessions at (a) 9:30 a.m., and (b) 6:30 p.m.

Table 3 shows that the single-session averages throughout the several performed campaigns assumed similar values around 450 ppm, ranging in between a minimum of 419 ppm and a maximum of 592 ppm. Nevertheless, between the total 16 sessions, two of these (session 5 at 9:30 a.m. and session 7 at 6:30 p.m.) were clearly out of the common concentration profile, presenting higher CO<sub>2</sub> concentration baseline, i.e., an average value of 524 and 592 ppm, respectively. This fact can be explained considering that both sessions were monitored during working days when the maximum flux was concentrated at rush hour.

**Table 3.** Statistical descriptors of datasets collected in each monitoring session.

9.30 am	Monitoring Session							
	1	2	3	4	5	6	7	8
Min [ppm]	290	330	360	260	350	190	160	290
Max [ppm]	620	710	570	600	800	750	700	790
Ave [ppm]	441	445	448	419	524	441	449	479
St. Dev. [ppm]	49	44	27	44	65	95	60	78
6.30 pm	1	2	3	4	5	6	7	8
Min [ppm]	350	300	310	230	260	350	340	390
Max [ppm]	610	540	660	620	560	610	1340	550
Ave [ppm]	458	442	425	430	419	462	592	469
St. Dev. [ppm]	38	35	44	51	41	27	205	27

For a better understanding, correlation to other physical parameters is here discussed.

CO<sub>2</sub> variability (i) in space for the whole 9:30 a.m. and 6:30 p.m. monitoring sessions, and (ii) during every single session are expressed simultaneously by graphs in Figure 3 on the *xz* and *yz* planes, respectively. Moreover, each observation was associated with the collected air temperature (Figure 3a,b) and wind speed (Figure 3c,d) values by color plots. The space variation, along the *x*-axis, is expressed in terms of absolute distance between the specific observation location and the starting point of the monitoring path in meters. Locations of the two crossroads are highlighted on the *xz* planes of the graphs.

The highest peaks of CO<sub>2</sub> were observed during monitoring session 7 at 6:30 p.m. when the collected dataset standard deviation rose up to 205 ppm. The CO<sub>2</sub> peaks were detected in the proximity of the Northern crossroads and at the beginning of the monitoring path, i.e., when the operator was still in the Southern square. Moreover, such CO<sub>2</sub> peaks occurred almost simultaneously with the highest detected air temperatures and low values of wind speed, responsible for buoyancy and stagnation.

The same Figure 3a,b also shows interesting data in terms of air-temperature overheating. An increase in air temperature was registered during the afternoons when a more compact temperature distribution was monitored, imputable to local anthropogenic actions. In fact, morning air temperature was still dependent on weather conditions, which were relatively buffered in the afternoons due to UHI perceived at the pedestrian level. The only exception is the monitoring number 7, when both the morning and the afternoon sessions showed comparable values with an average temperature of 18.2 °C and 17.7 °C, respectively. This condition could be imputed to hotter conditions experienced during the day, able to dominate the local UHI effect.

Figure 4 shows the CO<sub>2</sub> concentration with respect to both air temperature (Figure 4a) and wind speed (Figure 4b), considering the whole collected data to better underline possible existing correlations among the presented data. The CO<sub>2</sub> dispersion fluctuated around the average value, i.e., 459 ppm, representative of the monitored area level of pollution. CO<sub>2</sub> values above 1000 ppm were observed only for air temperatures between 17.6 °C and 19.0 °C and wind speed below 1.3 m/s, suggesting the occurrence of air stagnation.

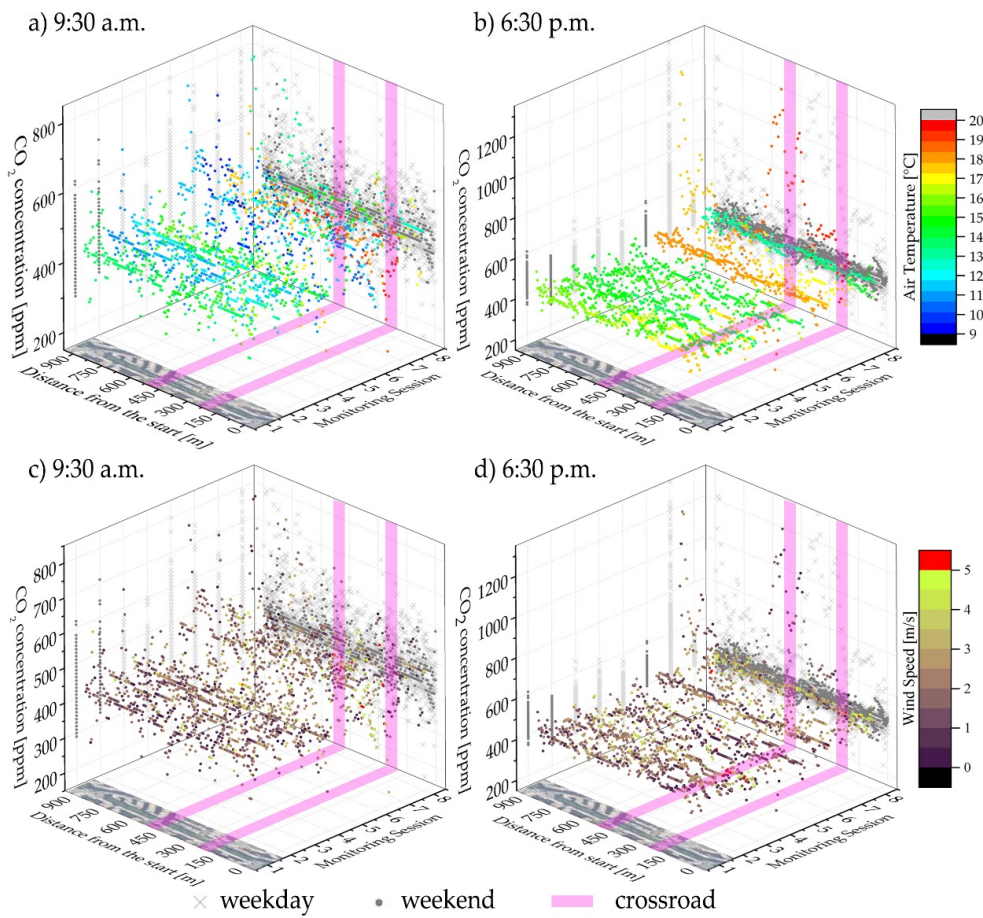


**Figure 3.** CO<sub>2</sub> concentration and air temperature with respect to the distance from the starting point for each session conducted at (a) 9.30 am and (b) 6.30 p.m.; CO<sub>2</sub> concentration and wind speed with respect to the distance from the starting point for each session conducted at (c) 9:30 a.m. and (d) 6:30 p.m.

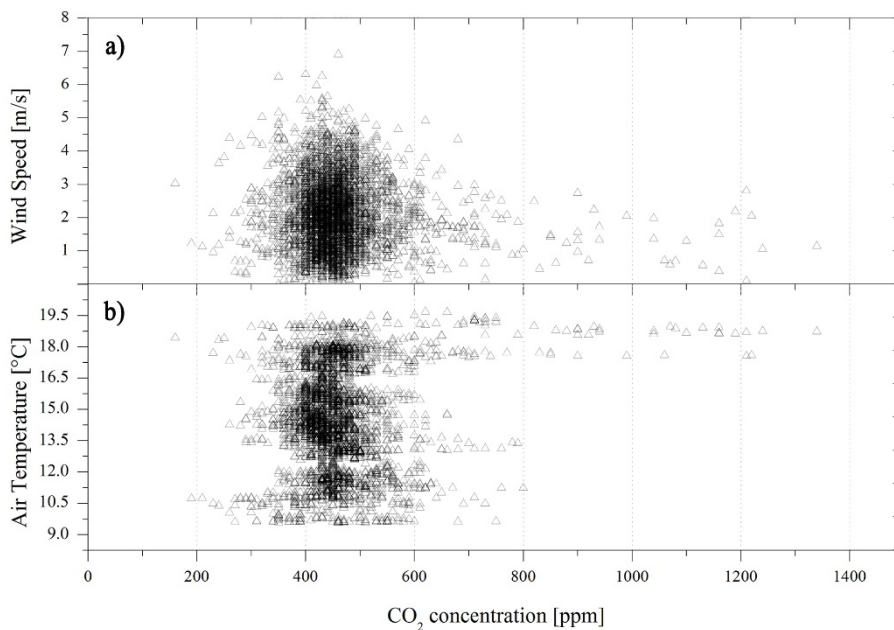


**Figure 4.** CO<sub>2</sub>-concentration distribution with respect to (a) wind speed and (b) air temperature for the whole collected data.

The detected CO<sub>2</sub> dispersion across the monitored road is statistically analyzed in Figure 5, by taking into account the two day-time monitoring sessions, i.e., 9:30 a.m. and 6:30 p.m., and distinguishing between working days and weekends. The continuous horizontal lines in the graphs represent CO<sub>2</sub> data range out of what observations can be considered outliers. In particular, outliers were defined from the interquartile range (IQR), which is the difference between the third (Q<sub>3</sub>) and the first (Q<sub>1</sub>) quartile of the dataset, i.e., 75th and 25th percentiles, respectively, as reported in Figure 5.

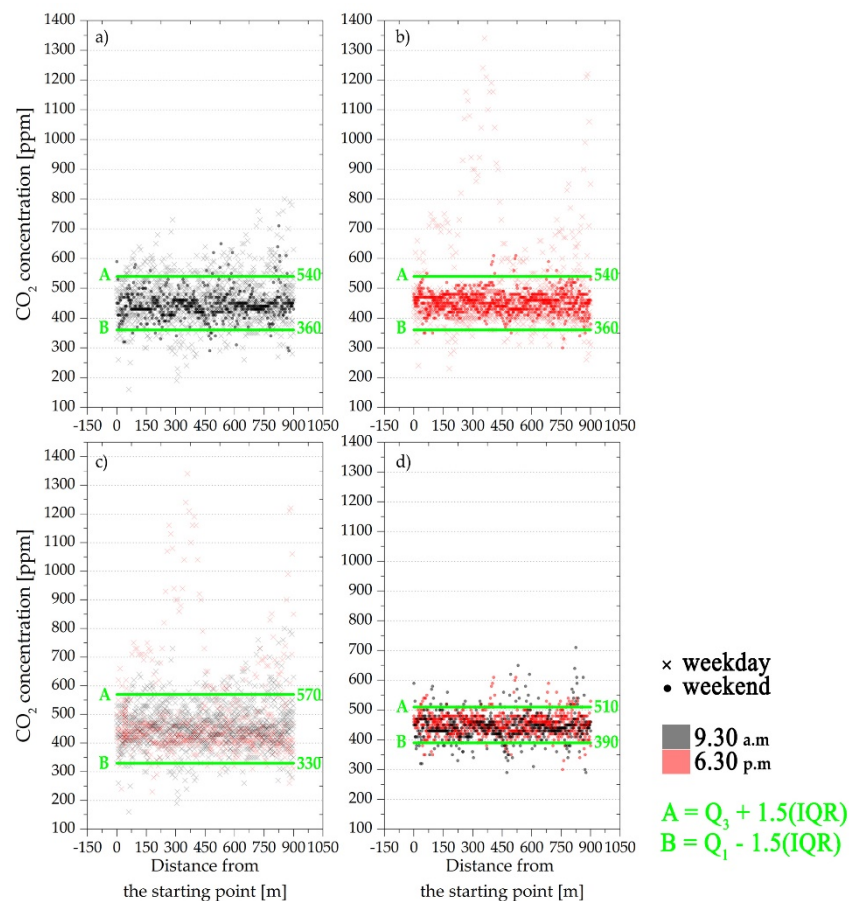


**Figure 5.** CO<sub>2</sub> distribution with respect to the latitude of the (a) 9:30 a.m., (b) 6:30 p.m., (c) weekdays, and (d) weekends monitoring sessions.

The monitoring sessions performed in the morning and in the afternoon did not show any significant differences in terms of the sample distribution. The upper and lower outlier limits were the same for both obtained datasets, i.e., 360 and 540 ppm, respectively. On the other hand, the collected CO<sub>2</sub> range seemed less disperse during the weekends with respect to weekdays. Therefore, the peak daily hours may be defined as having similar air quality conditions, even if they are characterized by different levels of UHI, as previously shown. These observations were in line with the choice of the monitoring times as the two traffic rush hours throughout a working day. In addition, the weekday traffic may be responsible for important peaks of CO<sub>2</sub>-concentration increase, which were not visible during the weekends, where the anthropogenic action in terms of CO<sub>2</sub>-concentration increase was more compact and narrowly distributed.

## 5. Conclusions

The study of physical environmental parameters influencing the pollutant dispersion in urban areas plays a key role in achieving the main sustainable goals that are fixed in the 2030 Agenda for

Sustainable Development. These variables are also important for determining population well-being in urban areas affected by anthropogenic actions, responsible for urban heat island and local climate change. In this view, this work presents the original results coming from the novel adoption of a wearable sensing device meant to map environmental parameters' (including CO<sub>2</sub> concentration) spatial distribution in the urban environment from the pedestrian perspective. Citizens have an active role in environmental mapping of the urban spaces. The above-mentioned device was placed on a common bike helmet and the environmental information collected by the system was linked to geographic coordinates by means of a GPS antenna embedded in the compact experimental apparatus. The performed monitoring campaign consisted of several repetitions of the same path at traffic rush hours on both working days and weekends. In particular, the selected case study was a two-way, two-lane road in Rome, and 16 monitoring sessions were performed in total throughout one month, that is, eight at 9:30 a.m. and eight at 6:30 p.m. Collected CO<sub>2</sub>-concentration values were therefore correlated to timing, position, and other environmental parameters affecting pedestrians' well-being in the outdoors.

Data analysis showed that CO<sub>2</sub> concentration was generally around 450 ppm in the area. The pollutant dispersion was quite homogeneous along the road, while peaks were observed during only a few performed monitoring sessions. Rare concentration peaks, that is, up to 1340 ppm, meant the temporary presence of punctual sources of CO<sub>2</sub> or, referring to traffic flow, vehicle accelerations/congestions on working days. This assumption was confirmed by peak spatial distribution: they were located almost in proximity of the crossroads, regulated by both roundabouts and traffic lights. Therefore, the wearable monitoring system demonstrated the ability to catch pedestrian exposure variability to vehicle exhaust gases with a high spatial and temporal resolution. The same CO<sub>2</sub> concentration was also investigated in parallel to the air temperature analysis along the path, which showed to be influenced by emitted anthropogenic heat during the afternoons, combined with UHI intensity exacerbation.

The complexity of the monitoring system, indeed, allows to simultaneously collect several environmental parameters and experimentally investigate existing correlations. In this work, the CO<sub>2</sub> concentration was then analyzed with respect to air temperature and wind speed. None of the investigated correlations was found to be of statistical relevance, even if reasonable observations were carried out. For instance, CO<sub>2</sub> levels above 1000 ppm were observed only in relatively high air temperatures, that is, ranging between 17.6°C and 19.0°C, and low wind speed, that is, below 1.3 m/s, suggesting the occurrence of air stagnation. Finally, differences between weekday and weekend measures were analyzed. The dataset collected during weekends was more concentrated around the average, 450 ppm for both datasets. The monitored area was, indeed, less congested than during the weekends.

The experimental analysis and data assessment showed that the innovative methodology can provide further insight into people's well-being in an urban environment, where several variables affecting people's health and city livability may be correlated and need to be monitored at a specific pedestrian level in order to identify realistic risk and vulnerability maps. Therefore, further size reduction of the proposed tool and its diffusion among citizens may provide new opportunities and perspectives to extensively monitor and improve the life quality of pedestrians, influenced by poor air quality and local overheating, especially in a very dense and polluted city such as Rome.

As a future development to push forward effective exploitation of wearable monitoring systems, further monitoring campaigns will be planned in order to compare data collected in (i) different areas of the same city or (ii) the same types of outdoor spaces but located in different geographical areas. Final optimal configuration of combined monitoring strategies (e.g., weather stations, satellite measurements, and portable wearable instruments) for detecting microclimate granularity within the urban areas is the final ambition of this research.

**Author Contributions:** All of the authors worked on the conceptualization, data analysis, and writing and/or revising the manuscript versions. I.P. made the largest writing contribution, G.M. performed the field tests, A.L.P. was in charge of the funding management and revision. All authors have read and agreed to the published version of the manuscript.

**Funding:** The authors' acknowledgements are due to the European Union's Horizon 2020 program under grant agreement No 678407 (ZERO-PLUS) and to the Italian project SOS-CITTA supported by Fondazione Cassa di Risparmio di Perugia under the grant agreement 2018.0499.026.

**Acknowledgments:** The authors' acknowledgements are due to the European Union's Horizon 2020 program under grant agreement No 678407 (ZERO-PLUS) and to the Italian project SOS-CITTA supported by Fondazione Cassa di Risparmio di Perugia under the grant agreement 2018.0499.026.

**Conflicts of Interest:** The authors declare no conflict of interest.

## References

- 2018 Revision of World Urbanization Prospects | Multimedia Library—United Nations Department of Economic and Social Affairs. Available online: <https://www.un.org/development/desa/publications/2018-revision-of-world-urbanization-prospects.html> (accessed on 5 February 2020).
- Shukla, A.; Jain, K. Critical analysis of rural-urban transitions and transformations in Lucknow city, India. *Remote Sens. Appl. Soc. Environ.* **2019**, *13*, 445–456. [CrossRef]
- Xiao, H.; Kopecká, M.; Guo, S.; Guan, Y.; Cai, D.; Zhang, C.; Zhang, X.; Yao, W. Responses of Urban Land Surface Temperature on Land Cover: A Comparative Study of Vienna and Madrid. *Sustainability* **2018**, *10*, 260. [CrossRef]
- Silva, J.S.; da Silva, R.M.; Santos, C.A.G. Spatiotemporal impact of land use/land cover changes on urban heat islands: A case study of Paço do Lumiar, Brazil. *BUILD. Environ.* **2018**, *136*, 279–292. [CrossRef]
- Levi, Y.; Dayan, U.; Levy, I.; Broday, D.M. On the association between characteristics of the atmospheric boundary layer and air pollution concentrations. *Atmos. Res.* **2020**, *231*, 104675.
- Yang, B.; Yang, X.; Leung, L.R.; Zhong, S.; Qian, Y.; Zhao, C.; Chen, F.; Zhang, Y.; Qi, J. Modeling the Impacts of Urbanization on Summer Thermal Comfort: The Role of Urban Land Use and Anthropogenic Heat. *J. Geophys. Res. Atmos.* **2019**, *124*, 6681–6697. [CrossRef]
- WHO. *United Nations Millennium Development Goals*; WHO: Geneva, Switzerland, 2015.
- United Nations Sustainable Development Goals. Available online: <https://sustainabledevelopment.un.org/sdgs> (accessed on 4 July 2019).
- Shen, L.; Kyllö, J.; Guo, X. An integrated model based on a hierarchical indices system for monitoring and evaluating urban sustainability. *Sustainability* **2013**, *5*, 524–559. [CrossRef]
- Torgal, F.P. *Nearly Zero Energy Building Refurbishment: A Multidisciplinary Approach*; Springer: Berlin/Heidelberg, Germany, 2013; ISBN 9781447155225.
- Qiu, G.; Song, R.; He, S. The aggravation of urban air quality deterioration due to urbanization, transportation and economic development—Panel models with marginal effect analyses across China. *Sci. Total Environ.* **2019**, *651*, 1114–1125. [CrossRef]
- Sorte, S.; Arunachalam, S.; Naess, B.; Seppanen, C.; Rodrigues, V.; Valencia, A.; Borrego, C.; Monteiro, A. Assessment of source contribution to air quality in an urban area close to a harbor: Case-study in Porto, Portugal. *Sci. Total Environ.* **2019**, *662*, 347–360. [CrossRef]
- Li, B.; Wang, F.; Yin, H.; Li, X. Mega events and urban air quality improvement: A temporary show? *J. Clean. Prod.* **2019**, *217*, 116–126. [CrossRef]
- Krellenberg, K.; Bergsträßer, H.; Bykova, D.; Kress, N.; Tyndall, K. Urban sustainability strategies guided by the SDGs—A tale of four cities. *Sustainability* **2019**, *11*, 1116. [CrossRef]
- United States Environmental Protection Agency. *Sources of Greenhouse Gas Emissions*; United States Environmental Protection Agency: Washington, DC, USA, 2018.
- Garceau, T.J. Impacts of roundabouts on urban air quality: A case study of Keene, New Hampshire, USA. *J. Transp. Heal.* **2018**, *10*, 144–155. [CrossRef]
- Schmitz, S.; Becker, S.; Weiand, L.; Niehoff, N.; Schwartzbach, F.; von Schneidmesser, E. Determinants of public acceptance for traffic-reducing policies to improve urban air quality. *Sustainability* **2019**, *11*, 3991. [CrossRef]

18. Hooftman, N.; Oliveira, L.; Messagie, M.; Coosemans, T.; Van Mierlo, J.; Hooftman, N.; Oliveira, L.; Messagie, M.; Coosemans, T.; Van Mierlo, J. Environmental analysis of petrol, diesel and electric passenger cars in a Belgian urban setting. *Energies* **2016**, *9*, 84. [[CrossRef](#)]
19. Yang, J.; Shi, B.; Zheng, Y.; Shi, Y.; Xia, G. Urban form and air pollution dispersion: Key index and mitigation strategies. *Sustain. Cities Soc.* **2019**, *57*, 101955. [[CrossRef](#)]
20. Pisoni, E.; Christidis, P.; Thunis, P.; Trombetti, M. Evaluating the impact of “Sustainable Urban Mobility Plans” on urban background air quality. *J. Environ. Manag.* **2019**, *231*, 249–255. [[CrossRef](#)]
21. Lin, B.; Zhu, J. Changes in urban air quality during urbanization in China. *J. Clean. Prod.* **2018**, *188*, 312–321. [[CrossRef](#)]
22. Lai, L.-W. The influence of urban heat island phenomenon on PM concentration: An observation study during the summer half-year in metropolitan Taipei, Taiwan. *Theor. Appl. Climatol.* **2018**, *131*, 227–243. [[CrossRef](#)]
23. Matthaios, V.N.; Kramer, L.J.; Sommariva, R.; Pope, F.D.; Bloss, W.J. Investigation of vehicle cold start primary NO<sub>2</sub> emissions inferred from ambient monitoring data in the UK and their implications for urban air quality. *Atmos. Environ.* **2019**, *199*, 402–414. [[CrossRef](#)]
24. Langford, N.J. Carbon dioxide poisoning. *Toxicol. Rev.* **2005**, *24*, 229–235. [[CrossRef](#)]
25. Kettner, M.; Ramsthaler, F.; Juhnke, C.; Bux, R.; Schmidt, P. A Fatal Case of CO<sub>2</sub> Intoxication in a Fermentation Tank. *J. Forensic Sci.* **2013**, *58*, 556–558. [[CrossRef](#)]
26. Gill, J.R.; Ely, S.F.; Hua, Z. Environmental Gas Displacement. *Am. J. Forensic Med. Pathol.* **2002**, *23*, 26–30. [[CrossRef](#)] [[PubMed](#)]
27. Cotana, F.; Vittori, S.; Marseglia, G.; Medaglia, C.M.; Coccia, V.; Petrozzi, A.; Nicolini, A.; Cavalaglio, G. Pollutant emissions of a biomass gasifier inside a multifuel energy plant. *Atmos. Pollut. Res.* **2019**, *10*, 2000–2009. [[CrossRef](#)]
28. Spinelle, L.; Gerboles, M.; Villani, M.G.; Aleixandre, M.; Bonavitacola, F. Field calibration of a cluster of low-cost commercially available sensors for air quality monitoring. Part B: NO, CO and CO<sub>2</sub>. *Sensors Actuators B Chem.* **2017**, *238*, 706–715. [[CrossRef](#)]
29. Arnfield, A.J. Review two decades of urban climate research: A review of turbulence, exchanges of energy and water, and the urban heat island. *Int. J. Climatol. Int. J. Clim.* **2003**, *23*, 1–26. [[CrossRef](#)]
30. Oke, T.R. The urban energy balance. *Prog. Phys. Geogr.* **1988**, *12*, 471–508. [[CrossRef](#)]
31. Jin, H.; Cui, P.; Wong, N.; Ignatius, M. Assessing the effects of urban morphology parameters on microclimate in Singapore to control the urban heat island effect. *Sustainability* **2018**, *10*, 206. [[CrossRef](#)]
32. Sarrat, C.; Lemonsu, A.; Masson, V.; Guedalia, D. Impact of urban heat island on regional atmospheric pollution. *Atmos. Environ.* **2006**, *40*, 1743–1758. [[CrossRef](#)]
33. Abbassi, Y.; Ahmadikia, H.; Baniyadi, E. Prediction of pollution dispersion under urban heat island circulation for different atmospheric stratification. *Build. Environ.* **2020**, *168*, 106374. [[CrossRef](#)]
34. Memon, R.A.; Leung, D.Y.C.; Liu, C.-H. An investigation of urban heat island intensity (UHII) as an indicator of urban heating. *Atmos. Res.* **2009**, *94*, 491–500. [[CrossRef](#)]
35. Piselli, C.; Castaldo, V.L.; Pigliautile, I.; Pisello, A.L.; Cotana, F. Outdoor comfort conditions in urban areas: On citizens’ perspective about microclimate mitigation of urban transit areas. *Sustain. Cities Soc.* **2018**, *39*, 16–36. [[CrossRef](#)]
36. Rosso, F.; Golasi, I.; Castaldo, V.L.; Piselli, C.; Pisello, A.L.; Salata, F.; Ferrero, M.; Cotana, F.; de Lieto Vollaro, A. On the impact of innovative materials on outdoor thermal comfort of pedestrians in historical urban canyons. *Renew. Energy* **2018**, *118*, 825–839. [[CrossRef](#)]
37. Zhang, X.; Steeneveld, G.-J.; Zhou, D.; Duan, C.; Holtslag, A.A.M. A diagnostic equation for the maximum urban heat island effect of a typical Chinese city: A case study for Xi’an. *Build. Environ.* **2019**, *158*, 39–50. [[CrossRef](#)]
38. Pakarnseree, R.; Chunkao, K.; Bualert, S. Physical characteristics of Bangkok and its urban heat island phenomenon. *Build. Environ.* **2018**, *143*, 561–569. [[CrossRef](#)]
39. Matzarakis, A.; Amelung, B. Physiological Equivalent Temperature as Indicator for Impacts of Climate Change on Thermal Comfort of Humans, Chapter 9. In *Seasonal Forecasts, Climatic Change and Human Health. Advances in Global Change Research, Vol 30*; Thomson, M.C., Garcia-Herrera, R., Beniston, M., Eds.; Springer: Dordrecht, The Netherlands, 2008.

40. Rizvi, S.H.; Alam, K.; Iqbal, M.J. Spatio-temporal variations in urban heat island and its interaction with heat wave. *J. Atmos. Solar-Terr. Phys.* **2019**, *185*, 50–57. [[CrossRef](#)]
41. Meehl, G.A.; Tebaldi, C. More intense, more frequent, and longer lasting heat waves in the 21st century. *Science* **2004**, *305*, 994–997. [[CrossRef](#)] [[PubMed](#)]
42. Zhao, L.; Oppenheimer, M.; Zhu, Q.; Baldwin, J.W.; Ebi, K.L.; Bou-Zeid, E.; Guan, K.; Liu, X. Interactions between urban heat islands and heat waves. *Environ. Res. Lett.* **2018**, *13*, 034003. [[CrossRef](#)]
43. Sun, R.; Lü, Y.; Yang, X.; Chen, L. Understanding the variability of urban heat islands from local background climate and urbanization. *J. Clean. Prod.* **2019**, *208*, 743–752. [[CrossRef](#)]
44. Gu, Y.; Li, D. A modeling study of the sensitivity of urban heat islands to precipitation at climate scales. *Urban Clim.* **2018**, *24*, 982–993. [[CrossRef](#)]
45. Jato-Espino, D. Spatiotemporal statistical analysis of the Urban Heat Island effect in a Mediterranean region. *Sustain. Cities Soc.* **2019**, *46*, 101427. [[CrossRef](#)]
46. Paolini, R.; Antretter, F.; Cotana, F.; Pisello, A.L.; MeshkinKiya, M.; Zani, A.; Poli, T.; Castaldo, V.L. The hygrothermal performance of residential buildings at urban and rural sites: Sensible and latent energy loads and indoor environmental conditions. *Energy Build.* **2016**, *152*, 792–803. [[CrossRef](#)]
47. Parece, T.E.; Li, J.; Campbell, J.B.; Carroll, D. Assessing urban landscape variables' contributions to microclimates. *Adv. Meteorol.* **2016**, *2016*, 8736263. [[CrossRef](#)]
48. Mofarrah, A.; Husain, T. A holistic approach for optimal design of air quality monitoring network expansion in an urban area. *Atmos. Environ.* **2010**, *44*, 432–440. [[CrossRef](#)]
49. Vuckovic, M.; Kiesel, K.; Mahdavi, A. The extent and implications of the microclimatic conditions in the urban environment: A Vienna case study. *Sustainability* **2017**, *9*, 177. [[CrossRef](#)]
50. Cunha-Lopes, I.; Martins, V.; Faria, T.; Correia, C.; Almeida, S.M. Children's exposure to sized-fractioned particulate matter and black carbon in an urban environment. *Build. Environ.* **2019**, *155*, 187–194. [[CrossRef](#)]
51. Liu, T.; Zhu, Y.; Yang, Y.; Ye, F. ALC2: When Active Learning meets Compressive Crowdsensing for Urban Air Pollution Monitoring. *IEEE Internet Things J.* **2019**, *6*, 9427–9438. [[CrossRef](#)]
52. Xu, S.; Zou, B.; Lin, Y.; Zhao, X.; Li, S.; Hu, C. Strategies of method selection for fine-scale PM<sup>2.5</sup> mapping in an intra-urban area using crowdsourced monitoring. *Atmos. Meas. Tech.* **2019**, *12*, 2933–2948. [[CrossRef](#)]
53. Huang, J.; Duan, N.; Ji, P.; Ma, C.; Ding, Y.; Yu, Y.; Zhou, Q.; Sun, W. A Crowdsourced Sensing System for Monitoring Fine-Grained Air Quality in Urban Environments. *IEEE Internet Things J.* **2019**, *6*, 3240–3247. [[CrossRef](#)]
54. Domínguez, F.; Dauwe, S.; Cuong, N.T.; Cariolaro, D.; Touhafi, A.; Dhoedt, B.; Botteldooren, D.; Steenhaut, K. Towards an environmental measurement cloud: Delivering pollution awareness to the public. *Int. J. Distrib. Sens. Networks* **2014**, *10*, 541360. [[CrossRef](#)]
55. Dhingra, S.; Madda, R.B.; Gandomi, A.H.; Patan, R.; Daneshmand, M. Internet of things mobile-air pollution monitoring system (IoT-Mobair). *IEEE Internet Things J.* **2019**, *6*, 5577–5584. [[CrossRef](#)]
56. Pigliautile, I.; Pisello, A.L. A new wearable monitoring system for investigating pedestrians' environmental conditions: Development of the experimental tool and start-up findings. *Sci. Total Environ.* **2018**, *630*, 690–706. [[CrossRef](#)] [[PubMed](#)]
57. Pioppi, B.; Pigliautile, I.; Piselli, C.; Pisello, A.L. Cultural heritage microclimate change: Human-centric approach to experimentally investigate intra-urban overheating and numerically assess foreseen future scenarios impact. *Sci. Total Environ.* **2020**, *703*, 134448. [[CrossRef](#)] [[PubMed](#)]
58. Dhakal, S. Urban energy use and carbon emissions from cities in China and policy implications. *Energy Policy* **2009**, *37*, 4208–4219. [[CrossRef](#)]
59. Pigliautile, I.; Pisello, A.L. Environmental data clustering analysis through wearable sensing techniques: New bottom-up process aimed to identify intra-urban granular morphologies from pedestrian transects. *Build. Environ.* **2020**, *171*, 106641. [[CrossRef](#)]
60. Lee, J.; Kim, D.; Ryoo, H.-Y.; Shin, B.-S. Sustainable wearables: Wearable technology for enhancing the quality of human life. *Sustainability* **2016**, *8*, 466. [[CrossRef](#)]
61. Snyder, E.G.; Watkins, T.H.; Solomon, P.A.; Thoma, E.D.; Williams, R.W.; Hagler, G.S.W.; Shelow, D.; Hindin, D.A.; Kilaru, V.J.; Preuss, P.W. The changing paradigm of air pollution monitoring. *Environ. Sci. Technol.* **2013**, *47*, 11369–11377. [[CrossRef](#)]
62. Jacobson, M.Z. Enhancement of Local Air Pollution by Urban CO<sub>2</sub> Domes. *Environ. Sci. Technol.* **2010**, *44*, 2497–2502. [[CrossRef](#)]

63. ARPA Lazio—Agenzia Regionale Protezione Ambientale del Lazio. Available online: <http://www.arpalazio.gov.it/> (accessed on 8 April 2020).
64. Jandacka, D.; Durcanska, D.; Kovalova, D. Concentrations of traffic related pollutants in the vicinity of different types of urban crossroads. *Commun.-Sci. Lett. Univ. Zilina* **2019**, *21*, 49–58.



© 2020 by the authors. Licensee MDPI, Basel, Switzerland. This article is an open access article distributed under the terms and conditions of the Creative Commons Attribution (CC BY) license (<http://creativecommons.org/licenses/by/4.0/>).